Driving simulator motion base right sizing

Ehsan Sadraei [1], Richard Romano [1], Samantha Jamson [1], Gustav Markkula [1], Hamish Jamson [1]

(1) Institute for transport studies, University of Leeds, United Kingdom, e-mail: {tses, r.romano, s.l.jamson g.markkula, a.h.jamson}@leeds.ac.uk

Abstract *– Driving simulator motion bases are available having various mechanisms and characteristics; among them, the synergistic 6DoF hexapod-type integrated with a sliding rail is the most commonly used. There is a large variety in workspaces (sizes) of both the hexapod and sliding rail used in research and training simulators, and there lacks consensus on what size of motion base is really needed in order to have high fidelity motion cueing. In this paper we introduce an approach that balances between having high fidelity motion cueing and at the same time addressing the minimum size requirement to reduce the purchase cost. A conventional classic motion cueing algorithm (MCA) is used together with an optimization method to establish the minimum workspace requirement, while meeting the fidelity criteria defined in literature. The right sizing requirements are driving task dependent, so in order to test this method, low and high motion-demanding driving tasks are tested using the experimental data collected from professional drivers. A standard (high) and a reduced (low) amount of tilt coordination is selected, showing how this defines a range of rail sizes to consider.*

Keywords: *motion cueing, fidelity corridor, sliding rail size.*

Introduction

In driving simulators, motion error can be defined as the difference between the position, velocity and acceleration of a real and simulated vehicle. The position and mostly velocity is perceived through the human visual system and can be represented quite accurately by the simulator visual cueing system; acceleration is perceived through the human vestibular system which the simulator motion base reproduces. The motion cueing fidelity criteria are usually defined based on an undetectable amount of motion errors and the border between when vestibular motion cues are no longer perceived by drivers to be synchronized with the visual motion cue are named the fidelity boundaries, corridors, or coherent zones.

The motion base characteristics and constraints cause the discrepancy between the real-virtual vestibular motion cues, and this affects the simulator motion cueing fidelity. Having a very large motion base can reduce the motion error, however the purchase costs of a motion base increases with the workspace size. For this reason there exists the question as to what motion base workspace is adequate to cut the costs but also to keep the fidelity of motion cueing acceptable.

The fidelity corridors are addressed in either open or closed loop methods. In the closed-loop case, drivers' subjective and objective behaviour data are collected during active driving (driver controls the vehicle) and correlated to the motion error to draw the fidelity corridors. In the open-loop method either passive driving is used (where the driver is not controlling the vehicle; i.e. is a passenger) collecting and correlating their subjective data to the motion error to draw the fidelity corridors, or no driver is involved, looking only at the dynamic response of motion system to certain inputs.

Motion error is usually evaluated in the time domain via amplitude error, or the frequency domain via gain and phase errors. In the closed-loop time domain, studies in large driving simulators have shown that motion that is objectively closer to the actual vehicle motion (one to one) in the given driving task is not always perceived as more realistic [Sav14, Ber13]. They considered a slalom driving task and consistently showed that scaled down motion between 0.4 and 0.75 of full motion is more realistic i.e. has higher fidelity.

In the first attempts of drawing the fidelity corridor in the frequency domain for helicopter simulators, a minimum undetectable distortion between the visual and motion cues was examined in open-loop. Only four phase and gain test points were examined for a tracking task with a frequency of 1 $\mathrm{rad/sec}$ where the human vestibular system has the highest perception gain [Sin77], see Fig. 1 dashed line. Later, using the same approach, Schroeder measured more test points and further modified the fidelity borders, the solid line [Sch99].

As we can see, a gain of 0.4 and a maximum phase error of 60 degrees will produce medium fidelity motion cues. However defining the three borders of low, medium and high fidelity is still an argument on how accurate the borders between them are, moreover in similar studies the fidelity corridors are

often defined only as fidelity and low fidelity areas. Hence, comparing Sinacori and Schroeder with other criteria explained next we can see the gain of 0.4 and phase of 60 degrees is an acceptable border of being in the fidelity zone.

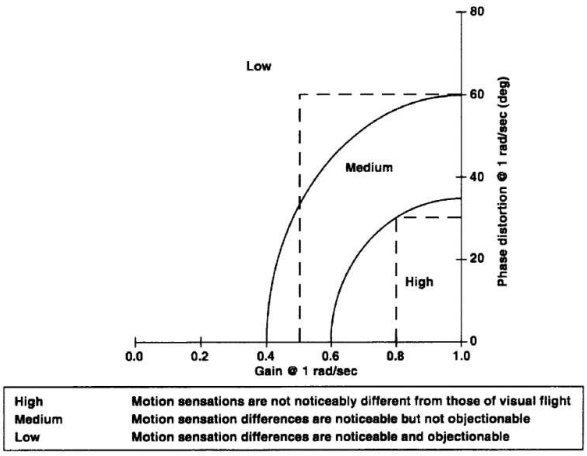

Figure 1. Sinacori (dashed line) and Schroeder (solid line) fidelity corridors for translational motion at 1 rad/sec, reproduced from [Sch99]

In more recent studies using Objective Motion Cueing Tests (OMCT) [Hos16] evaluated ten flight simulators to draw the corridors (named fidelity zones) on phase and gain plots in all degrees of freedom. They proposed an open-loop approach to avoid the ambiguity of the drivers' subjective assessments; objective measurements of the frequency response of the complete motion cueing system including the motion cueing algorithm (MCA) and motion base to a range of sinusoidal inputs frequency are tested and converted to Bode plots, as shown in Fig. 2. The dashed lines represent the fidelity corridors and are 2 standard deviations away from the mean value among all ten simulator tests. This method was adapted and tested in two driving simulators, and their performance approximately fit in the OMCT phase and gain corridors. Moreover they introduced further modifications to be added to the method for driving simulator evaluations [Fis16].

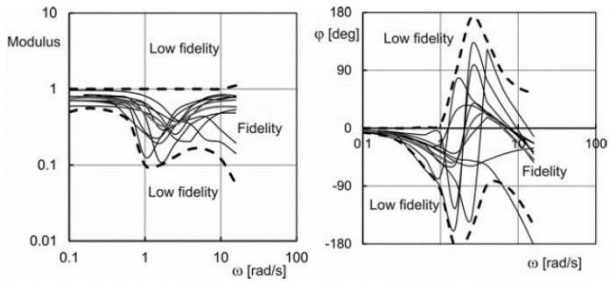

Figure 2. Fidelity corridor for lateral direction, modulus in $\mathrm{m/sec^2}$, reproduced from [Hos16]

In similar research, amplitude and phase coherence zones were defined as motion cue gain and phase attenuation that although not being a perfect match to the visual cue is still perceived by drivers to be coherent [Val13]. It has been shown that amplitude coherence is a function of magnitude and frequency of the visual cue, whereas the phase coherence is argued to be not, however further investigation was needed. To define the corridors, open-loop evaluations were used where subjects were requested to determine 'what is the strongest and weakest inertial motion amplitude that still matches the visual cue amplitude'. The experiments included flying manoeuvres and driving tasks.

Amplitude coherence zone for the lateral (sway) motions is represented in Fig. 3. It shows the amplitude coherence zones as coloured bars for two visual acceleration amplitudes of 0.5 and 1 $\mathrm{m/s^2}$ in three frequencies of 2, 3, 5 rad/s on the horizontal axis, and motion gain on the vertical axis. The range of bars shows the zones. The trends in the data shows that both the upper and lower threshold gains decrease slightly with increasing frequency and the gains are lower for the higher amplitude of the visual cue. The minimum gain for coherence zone on mean of all frequencies is about 0.6 for 0.5 $\mathrm{m/s^2}$, and about 0.4 for 1 $\mathrm{m/s^2}$. The phase coherence was found not to be affected by either the amplitude or the frequency of the stimuli, and 19 degrees of phase-error is reported for yaw and pitch DoFs on mean of all frequencies.

It is important to note that the accelerations available in driving tasks are usually higher than the1 $\mathrm{m/s^2}$ evaluated here, meaning that a lower minimum gain than 0.4 might be required for high acceleration demanding tasks. Moreover the phase corridor is only available for yaw DoF, requiring the maximum phase error of 19 degrees which might be different for translational DoFs.

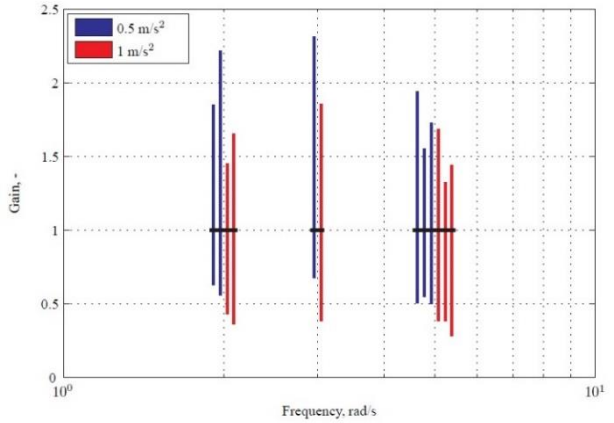

Figure 3. Coherence zones represented as the maximum and minimum motion gains obtained from the threshold values, across all amplitudes and all lateral motion. The horizontal black lines span different measurements made at the same visual amplitude, reproduced from [Val13]

Considering the represented fidelity criteria it is obvious there are two main factors defining the fidelity corridor, a) order of phase and gain distortion in each frequency and b) frequency range of interest that is most perceived by human. To find those and

draw the fidelity corridor we have looked at the acceleration amplitude and power spectral density (PSD) of input vehicle acceleration which drivers experience while driving, specifically for the data collected in a Driving Simulator Motion Cueing Assessment study [Sad17]. The study used eight drivers who performed a slalom (SLM) manoeuvre and driving through the so-called Land Rover handling track (LHT; a replica of a test track at the Revi test driving facilities in Northern Sweden). See the LHT track and SLM driving trajectory example in Fig. 4.

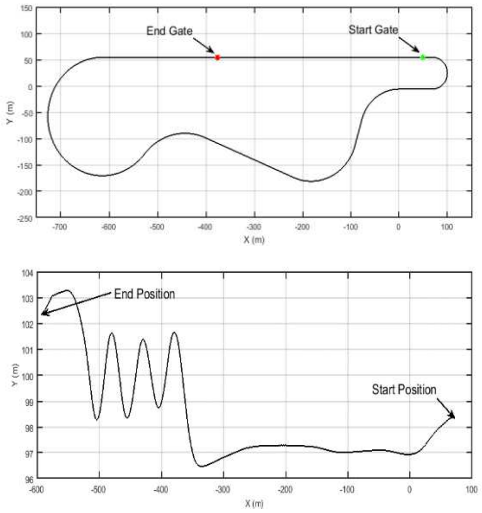

Figure 4. LHT track (top) and SLM (bottom) driving trajectory example

In each of the tasks the drivers were consecutively presented six motion configurations corresponding to permutations of three small, medium, large motion base sizes and two classic and mpc motion cueing algorithms, in a counter balanced order. They drove each of the configurations twice, so that in total there were 8 (drivers)*6 (configuration)*2 (repetition) equal to 96 data runs for each of the driving tasks.

Excluding the drivers' unsuccessful attempts (spin outs, etc.), an example of vehicle (model) lateral acceleration profile and the maximum absolute amplitude of the acceleration among all runs is shown in Fig. 5. To find the frequency range of interest, the acceleration was passed through a vestibular otolith model and the power spectral density (PSD) of it is shown in Fig. 6. The human perception threshold for translational accelerations is about 0.1 $\mathrm{m/s^2}$ (Nash et al., 2016) or $10 * \log_{10}\left(\frac{0.1}{\sqrt{2}}\right)^2 = -23$ db, the black dotted line is shown in Fig. 6. Its intersection with the perceived vehicle acceleration defines the frequency of interest it is the point where the acceleration is not perceptible by a driver at any higher frequency. The maximum frequency of interest is measured for all the data runs, see Fig. 6. For the LHT task it is 6.35 $\mathrm{rad/sec}$ and for the SLM is 9.28 $\mathrm{rad/sec}$.

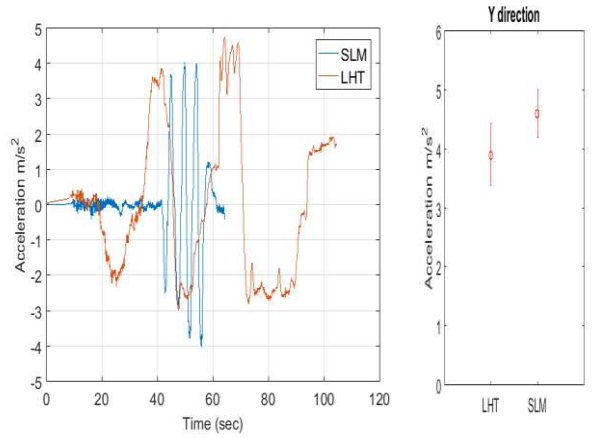

Figure 5. Vehicle model lateral acceleration, time series profile of an example run (left), and maximum amplitude of all runs with 95 percent confidence interval (right), for both LHT and SLM tasks.

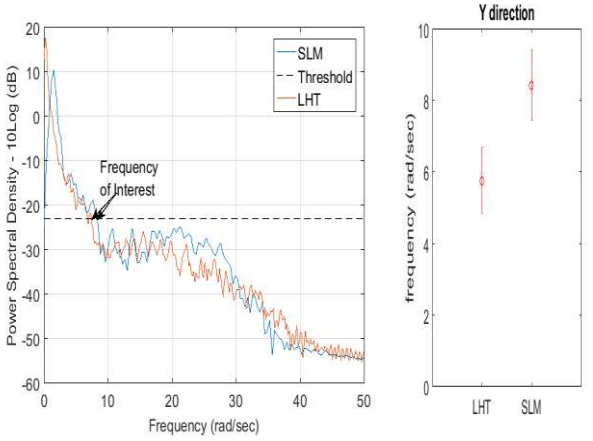

Figure 6. Perceived vehicle model lateral acceleration, power spectral density (left) of an example run, and maximum frequency of interest of all runs with 95 percent confidence interval (right), for both LHT and SLM tasks.

The fidelity corridor used later in optimizations, is the allowable gain and phase distortion and is chosen based on the intersection of all the represented fidelity criteria, shown in Fig. 7. Although the medium fidelity border of the Sinacori criteria (same as amplitude coherent zone) i.e. 0.4 (8 dB) of gain and 60 degrees of phase error is measured for a single frequency of 1 $\mathrm{rad/sec}$, here we assume it to be same for all frequencies as the green lines. We can see it fits within the range of OMCT fidelity zone for both gain and phase criteria and it is a more conservative corridor in middle range of frequencies compared to OMCT. For the phase at low frequency it is outer range, however as it is described later this is not of problem for our optimization fidelity corridor because the tilt coordination response fits within the OMCT corridor. Consequently the optimization corridor is selected similar to expanded Sinacori in frequency of interest as the yellow line, and is called fidelity corridor for remainder of the paper. Moreover, in OMCT and coherent zone studies there is no medium fidelity zone is defined, and it is either low or fidelity zones.

The frequency range of interest is chosen as 0.1 to 6.35 rad/sec for the LHT task, and 0.1 to 9.28 rad/sec for the SLM task, as can be seen in Fig. 7. Outside these ranges the gain and phase requirements are relaxed considerably. This helps the optimization problem to focus on minimizing error in the range of frequency of interest. The optimization corridors are drawn axisymmetric around the zero y axis in the interest range to minimize the errors to 0 dB and deg.

Using the generalised fidelity corridor, the next sections explain the motion cueing algorithm, the optimisation process and then apply the method on the experimental data to address the rail size requirement.

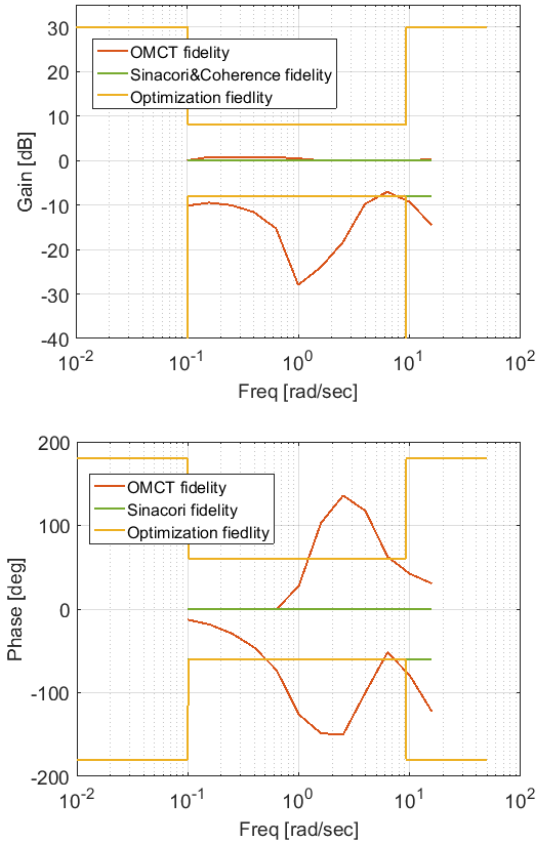

Figure 7. Fidelity corridors defined by OMCT, Sinacori, coherent zone and the one used in optimizations for LHT task

Methodology

Motion cueing

The classic MCA is a well-known motion cueing method developed by [Con70] with an updated layout introduced by [Rom17]. In its simplest form, for the longitudinal (X) and lateral (Y) translational degrees of freedom, it is the combination of second order high-pass and low-pass filters respectively for generating the translational and tilting accelerations as well as gains and limiters, Fig. 8. Simulator commanded acceleration a_s is related to input vehicle acceleration a_i as given in Eq. 1. However it includes coordinate transformations and higher order filters if washout[1] is required.

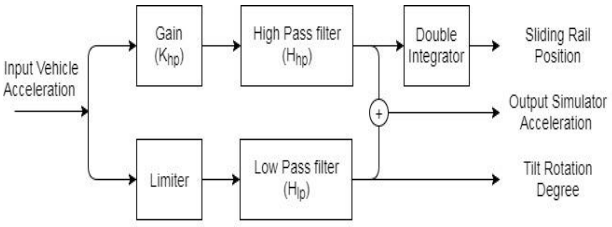

Figure 8. Classic motion cueing algorithm

$$\frac{a_s}{a_i} = \frac{k_{hp}s^2}{s^2+2\beta\omega_{hp}+{\omega_{hp}}^2} + \frac{{\omega_{lp}}^2}{s^2+2\beta\omega_{lp}+{\omega_{lp}}^2} \qquad (1)$$

The acceleration generated by the tilting depends on three parameters of tilting: maximum angle θ_{max} which is selected by limiter parameter a_{lim}, tilt angular velocity $\dot{\theta}_{max}$ and tilt angular acceleration $\ddot{\theta}_{max}$, selected by choosing the filter cut-off frequency ω_{lp} as in Eq. 2.

$$\frac{\ddot{\theta}_{max}\pi g}{180} = {\omega_{lp}}^2 \rightarrow \omega_{lp} \leq \sqrt{\frac{\ddot{\theta}_{max}\pi g}{180}}$$

$$\frac{\dot{\theta}_{max}\pi g}{180} = \frac{\omega_{lp}}{exp} \rightarrow \omega_{lp} \leq \frac{\dot{\theta}_{max}\pi g exp}{180} \qquad (2)$$

$$\frac{\theta_{max}\pi g}{180} = a_{lim} \rightarrow a_{lim} \leq \frac{\theta_{max}\pi g}{180}$$

The acceleration generated by the rail depends on two parameters of filter gain k_{hp} and cut-off frequency ω_{hp} which are related to sliding rail maximum excursion $x_{r,max}$ and maximum input vehicle acceleration $a_{i,max}$ as in Eq. 3. The selection of these parameters has a major impact on the motion cueing fidelity of the simulator.

$$\frac{k_{hp}a_{i,max}}{x_{r,max}} = {\omega_{hp}}^2 \rightarrow \omega_{hp} \geq \sqrt{\frac{k_{hp}a_{i,max}}{x_{r,max}}} \qquad (3)$$

Optimization

Using the available research providing the information on fidelity corridors, an automatic procedure for finding optimal MCA parameters

[1] During simulation time when input acceleration is constant and maximum excursion of rail is reached and washout brings back motion base to neutral position.

(without tilt coordination) was developed for finding the MCA parameters through a mathematical optimization method that minimizes the motion error while considering both the fidelity zones, and the motion base constraints [Sad16]. The optimization cost function is defined in Eq. 4 which minimizes sliding rail size and the acceleration error in time and frequency domain. W_0 to W_3 are the weights of cost function for time domain acceleration, gain and phase frequency domain and rail position errors.

$$\sum_{t=0}^{t_{sim}} w_0(a_s - a_i)^2 + \sum_{f \in f_{interest}} exp^{w_1(Gain_{now} - Gain_{corridorMax})} + exp^{-w_1(Gain_{now} - Gain_{corridorMin})} + \sum_{f \in f_{interest}} exp^{w_2(Phase_{now} - phase_{corridorMax})} + exp^{-w_2(phase_{now} - phase_{corridorMin})} + \sum_{f \in f_{interest}} exp^{w_3(RailPos_{now} - RailPos_{Max})} + exp^{-w_3(RailPos_{now} - RailPos_{Min})} \quad (4)$$

In this paper the methodology is extended to include tilt coordination as well as including another layer of optimization to define the minimum rail size. As a result, in the optimization an inner-loop runs the above sub-optimization to find if MCA parameters exist that meet the requirement for time and frequency domain corridor zones, and in an outer-loop 1 metre is added to the rail size beginning from 2 metres up to 30 metres. If the inner-loop optimization condition is met that size of rail is chosen, otherwise the outer-loop adds another metre until the corridor zone conditions are met, see Fig .9.

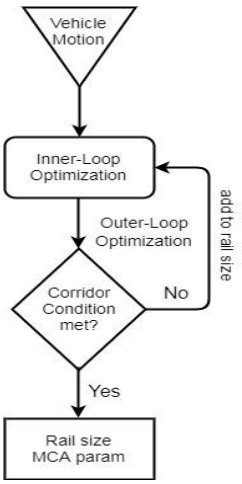

Figure 9. Optimization process

In the inner-loop optimization the tilt parameters play a critical role on how big the rail size should be. The tilt angle limits acceleration represented by tilting, and angular velocity (rate) and acceleration limits build-up of tilt acceleration which results in a larger sliding rail size to compensate, i.e. lower tilt parameters need bigger rail size and vice versa. The tilt degree is reported to be used up to 8 deg (equivalent to 1.37 $\mathrm{m/s^2}$), tilt angular velocity up to 7 $\mathrm{deg/s}$ and tilt angular acceleration up to 30 $\mathrm{deg/s^2}$. In a subjective comparison between ranges of tilt parameters for the slalom driving task, a tilt rate of 6 $\mathrm{deg/s}$ and 8 $\mathrm{deg/s^2}$ was found to be an acceptable set of parameters [Col16]. However they only considered two tilt acceleration of 8 and 30 $\mathrm{deg/s^2}$, and there might be a more optimal value in between.

Selecting a full range of tilt velocity and acceleration values is only possible by introducing the nonlinear rate limiters in the MCA model which needs further nonlinear frequency analysis to be used in the optimization. Consequently, relying on the typically used linear low-pass filter gives us little freedom on selecting a range of tilt values. Two sets of parameters for tilting were chosen as given in Tab. 1. These settings could be regarded as the interval of tilt motion allowance used in driving simulators, and representative of the maximum and minimum of sliding rail size requirement. In both of the settings the maximum represented acceleration is 1 $\mathrm{m/s^2}$ at unity gain due to $\theta_{\max}$ of 6 deg.

Table 1. Tilting parameters used for optimizations

Tilting parameters	High - ω_{lp} 2 rad/s	Low - ω_{lp} 1.17 rad/s
$\theta_{\max}$ (deg)	6	6
$\dot{\theta}_{\max}$ (deg/s)	4.3	2.51
$\ddot{\theta}_{\max}$ (deg/s^2)	23.5	8

Results and Discussion

Data from all the runs excluding outliers were tested to see how variable the minimum rail size requirement was among all drivers, configurations and repetitions. In the optimization process the high-pass filter parameters were calculated once per run and each tilt settings that meets the fidelity criteria and then the motion base size is calculated. The results of the optimizations for the LHT task is shown in Fig. 10, for the higher tilt limit a rail size of 7 (±3.5) metre meets the fidelity requirement for most of the runs, while it goes up to 20 (±10) metre with the lower tilt limit. Similarly for the SLM task Fig .11 the rail size required is in range of 2 (±1) to 4 (±2) metre for the higher and lower tilt limits.

The obtained optimization result shows the median high-pass filter cut-off frequency ω_{hp} is 0.57 to 0.98 $\mathrm{rad/sec}$ and gain of 0.83 to 0.9 for the low and high tilt limits in the LHT task; and for the SLM task the cut-off frequency of 0.41 to 0.69 $\mathrm{rad/sec}$ and gain of

0.68 to 0.64 for the low and high tilt limits, see Fig. 12. In each of the tasks the high-pass filter cut-off frequency ω_{hp} increases from low to high low-pass filter tilt setting (cut-off frequency), which also allows higher gain k_{hp} values. The gain k_{hp}values are lower for SLM than LHT because the vehicle maximum accelerations are higher for SLM than LHT, hence requires lower high-pass gain to fit within gain fidelity corridor.

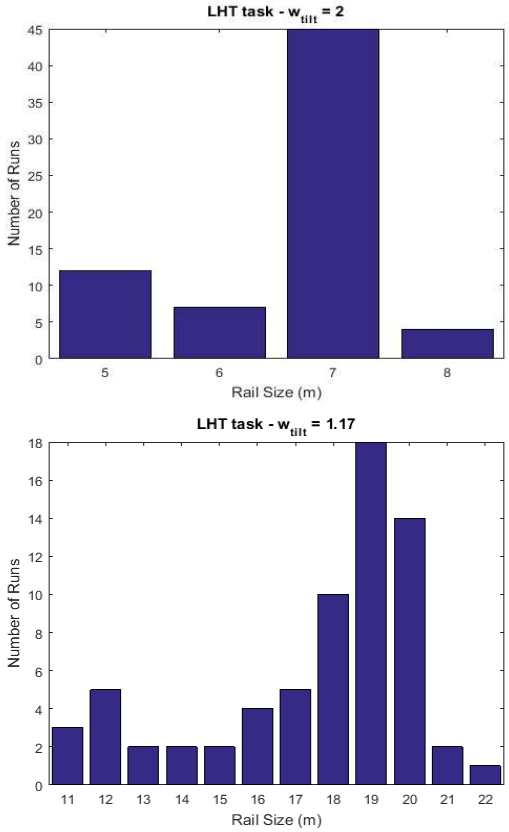

Figure 10. Optimization results for the LHT task with tilt setting high (top) and low (bottom). The bars show number of recorded runs that would require a given rail size

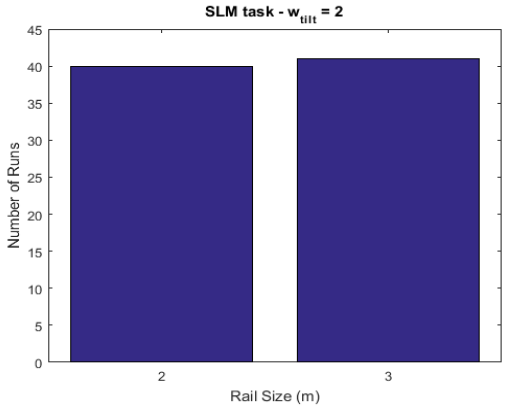

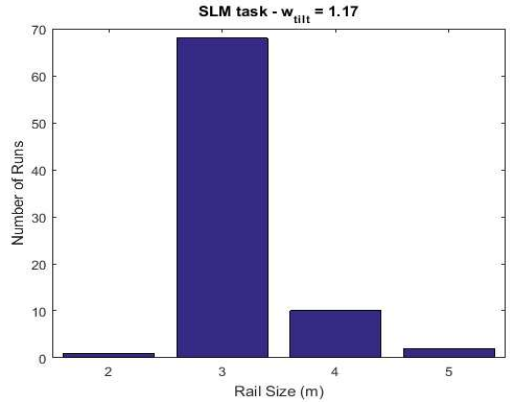

Figure 11. Optimization results for the slalom task with tilt limits high (top) and low (bottom). The bars show the number of recorded runs that would require a given rail size.

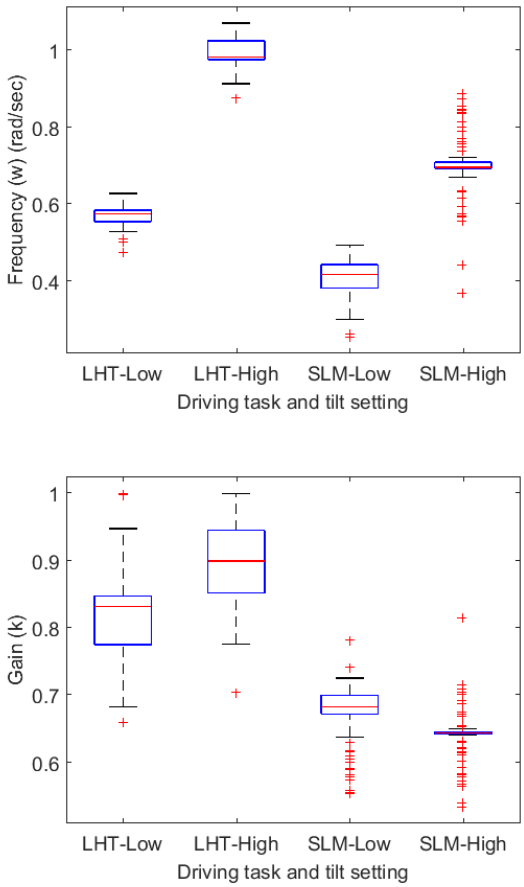

Figure 12. Optimization results for frequency ω_{hp} (top) and gain k_{hp} (bottom) range, for both driving tasks

For a single run of the LHT, the time domain response of acceleration, velocity and position of MCA output (the motion base set-points) is presented in Fig. 13. In addition the frequency domain response is shown where the total acceleration phase and gain response meets the fidelity criteria.

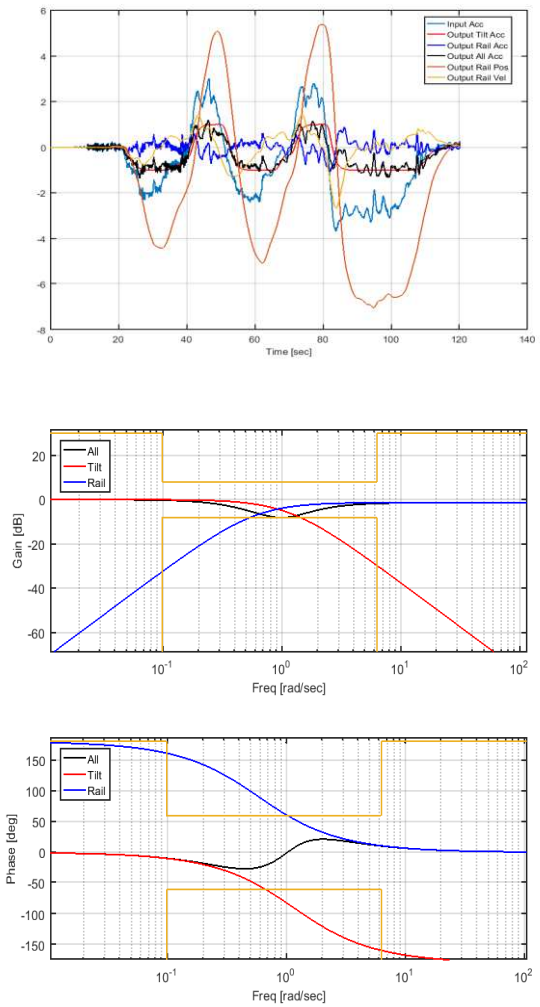

Figure 13. . Example of run optimization results for the LHT, high tilt limit, time domain repsonse of acclerations, velocity and position (top) and frequency domain response of acceleration (bottom)

Conclusions

A driving simulator motion base right sizing method is developed and represented in this paper. It is a specifically designed optimization method that searches for minimum motion base sliding rail size while keeping the motion cueing within the fidelity corridor. Different motion fidelity criteria are reviewed and a reasonable fidelity corridor is selected and used in the optimizations. The reliance on tilting for motion cueing plays a significant role in rail size requirement to keep the motion cueing within the fidelity corridors.

Two possible tilt parameter sets were considered which drive a minimum and maximum sliding rail size requirement. The method is tested for lateral motion of two low friction vehicle testing manoeuvres, considered by means of a large data set of recordings from professional drivers. For the Land Rover handling track a rail size range of 7 (±3.5) to 20 (±10) metre is required to meet the fidelity corridor for lateral motion cueing. For the Slalom this range is between 2 (±1) to 3 (±1.5) metres. It might be possible to further decrease the size requirement while maintaining fidelity using the model predictive method (mpc) motion cueing algorithm.

The focus here has been on lateral motion, however the motions in other DoFs also need to be generated by the simulator motion base and can be addressed with a similar optimisation method as the one developed here. Commonly, a hexapod is used to generate the rotational (roll, pitch and yaw) and vertical (heave) motions of vehicle, and again the same question of 'what workspace does it need to generate motion within the fidelity corridors?'

Roll, pitch, and heave are generally not a major concern. The collected data of various vehicle manoeuvres on flat ground shows the roll and pitch motions of vehicle never exceed ±5 degrees, in addition to a tilt degree of ±8 degree for each direction, both resulting in ±13 which can be represented one to one by a typical hexapod. The vertical (heave) motion of the vehicles is in range if 16 cm on flat surface, and could be represented one to one by a normal hexapod.

With regards to yaw motion, depending on the driving manoeuvres a full 360 degrees of motion might be used, which usually couldn't be represented one to one other than including a turntable for generating that motion, or again an MCA should be included.

As soon as an MCA is introduced for motion cueing a similar optimization process as described here is then needed to find the minimum workspace requirement in the relevant directions to generate motion within the corresponding fidelity corridors. However more research is needed specifically in driving simulators to address the fidelity corridors in each DoFs and their cross couplings.

Acknowledgments

This work was supported by Jaguar Land Rover and the UK-EPSRC grant EP/K014145/1 as part of the jointly funded Programme for Simulation Innovation.

References

BERTHOZ, A., BLES, W., BÜLTHOFF, H. H., GRÁCIO, B. C., FEENSTRA, P., FILLIARD, N., HÜHNE, R., KEMENY, A., MAYRHOFER, M. & MULDER, M. **Motion scaling for high-performance driving simulators**. *IEEE Transactions on Human-Machine Systems,* 2013, 43**,** 265-276.

COLOMBET, F., FANG, Z. & KEMENY, A. **Tilt thresholds for acceleration rendering in driving simulation**. *SAGE Journals SIMULATION,* 2016, 93**,** 595-603.

CONRAD, B. & SCHMIDT, S. 1970. **Motion drive signals for piloted flight simulators**. *NASA Technical Reports Server (NTRS),* 1970, 19700017803

FISCHER, M., SEEFRIED, A. & SEEHOF, C. **Objective Motion Cueing Test for Driving Simulators**. *Proceedings of the DSC 2016,* 07-09 Sep, Paris, France.

HOSMAN, R. & ADVANI, S. **Design and evaluation of the objective motion cueing test and criterion.** *The Aeronautical Journal,* 2016, 120**,** 873-891.

NASH, C. J., COLE, D. J. & BIGLER, R. S. **A review of human sensory dynamics for application to models of driver steering and speed control.** *Biological cybernetics,* 2016, 110**,** 91-116.

ROMANO, R., SADRAEI, E. & MARKKULA, G. **Rapid Tuning of the Classical Motion Cueing Algorithm.** *Proceedings of DSC 2017*. 06-08 Sep, Stuttgart, Germany.

SADRAEI, E., MARKKULA, G., ROMANO, R., TOMLINSON, A., HORROBIN, A., JAMSON, H., BEAN, A. & CHAPPELL, P. 2017. **PSI Theme 3 Milestone 3.5.6a Deliverable: Driving Simulator Motion Cueing Assessment.**

SADRAEI, E., ROMANO, R., ADVANI, S., JAMSON, A., CHAPPELL, P., MARKKULA, G., BEAN, A. & BOER, E. 2016. **Understanding Cue Utility in Controlled Evasive Driving Manoeuvres: Optimizing Vestibular Cues for Simulator & Human Abilities.** *IFAC-PapersOnLine,* 2016, 49**,** 414-419.

SAVONA, F., STRATULAT, A. M., DIAZ, E., HONNET, V., HOUZE, G., VARS, P., MASFRAND, S., ROUSSARIE, V. & BOURDIN, C. **The Influence of Lateral, Roll and Yaw Motion Gains on Driving Performance on an Advanced Dynamic Simulator.** *The Sixth International Conference on Advances in System Simulation.* 2014.

SCHROEDER, J. A. **Helicopter flight simulation motion platform requirements.** NASA Technical Reports Server (NTRS). 1999, 19990080926

SINACORI, J. B. **The determination of some requirements for a helicopter flight research simulation facility.** *NASA Technical Reports Server (NTRS),* 1977, NASA-CR-152066, TR-1097-1.

VALENTE PAIS, A. **Perception Coherence Zones in Vehicle Simulation.** *PhD thesis, Delft University of Technology,* 2013.